Institute of Space and Aeronautical Science, University of Tokyo
Report No. 511, March 1974

An Analysis of Shock Waves in Binary Gas Mixtures with Special Regard to Temperature Overshoot**

By

Kanji ABE* and Hakuro OGUCHI

Summary: Shock wave structures in argon-helium mixtures are numerically analysed on the basis of a kinetic model for binary gas mixtures. The results are compared with Harnett and Muntz' experiment, and reasonable agreement between computation and experiment is found. Special attention is paid to the overshoot phenomena of argon temperature. The argon temperature overshoot is shown from the results to occur for a sufficiently small mole fraction of argon. Such overshoot is also shown to occur for a comparatively larger mole fraction of argon, as the shock Mach number becomes higher.

1. INTRODUCTION

A number of widely varying studies of shock wave structures in binary gas mixtures have been made over the last decade. Sherman considered the shock wave structures employing a continuum approach, especially emphasizing the effect of mutual diffusions in binary gas mixtures [*1*]. A notable feature of this study was that Sherman showed a possibility of a trace element of heavy gas having a velocity above its upstream value. This anomalous velocity overshoot, which was called the Sherman anomaly, stimulated the subsequent studies, but was eliminated by the subsequent theoretical [*2–7*] and experimental [*8–9*] studies. On the other hand, these studies brought to light other new and interesting phenomena. Among these is a possibility that for the case where the mole fraction of heavy gas is small, the heavy gas temperature does not show a monotonic increase in the shock wave structure, but overshoots the Rankine-Hugoniot downstream value [*3–5*].

Recently, Harnett and Muntz conducted an experiment on the shock wave structures in argon-helium mixtures by using the electron fluorescence technique together with the Doppler broadening technique [*10*]. Their experiment inovlved measuring the distribution function of each species of the mixture. They studied the three shock waves where the argon mole fractions are 0.115, 0.247 and 0.44, and the shock Mach number was fixed at approximately 1.6 in each of the three cases. The experiment indicated no argon temperature overshoot even for the smallest argon

* Department of Applied Science, Faculty of Engineering, Kyushu University.

** This work was done while the first author was Kyodo-Kenkyuin (cooperative research fellow) of Institute of Space and Aeronautical Science, University of Tokyo.

mole fraction: $\chi_A=0.115$. This fact seems to be contrast to the computational results. So far no computational datum for the same condition as the experiment is available. For comparison with the experiment, in this work the computations based on a kinetic model [*11, 12*] are made for the same condition as the experiment by Harnett and Muntz. In order to clarify the overshoot phenomena of heavy gas temperature, computations are also made for the case where $\chi_A=0.01$ and the shock Mach number $M=1.6$, and for the case where $\chi_A=0.1$ and $M=3.0$.

2. Fundamental Equations

For a steady one-dimensional motion the kinetic model equations for binary gas mixtures are

$$u\partial f_i/\partial x=\nu_{ii}(M_{ii}-f_i)+\nu_{ij}(M_{ij}-f_i), \qquad (i, j=1, 2,\ i\neq j), \qquad (1)$$

where the collision frequencies ν_{ii} and ν_{ij} are expressed as

$$\nu_{ii}=2\pi(0.422)(2B_{ii}/m_i)^{1/2}n_i, \qquad \nu_{ij}=2\pi(0.422)[(m_i+m_j)B_{ij}/m_im_j]^{1/2}n_j,$$

if the molecules are assumed to obey the Maxwell force law (intermolecular forces are given by $F_{ii}=B_{ii}/r^5$ and $F_{ij}=B_{ij}/r^5$). The first term of the right-hand side of Eq. (1) is the BGK collision model for self-collision. The quantity M_{ii} is the Maxwellian distribution defined by

$$M_{ii}=n_i(m_i/2\pi\kappa T_i)^{3/2}\exp\left[-m_i(\boldsymbol{v}-U_i\boldsymbol{i})^2/2\kappa T_i\right],$$

where $\boldsymbol{i}$ is the unit vector parallel to the x-axis, and $\boldsymbol{v}=(u, v, w)$ the particle velocity. The second term represents cross-collisions and M_{ij} is a Maxwellian distribution given by

$$M_{ij}=n_i(m_i/2\pi\kappa T_{ij})^{3/2}\exp\left[-m_i(\boldsymbol{v}-U_{ij}\boldsymbol{i})^2/2\kappa T_{ij}\right],$$

where the quantities U_{ij} and T_{ij} are related to U_i, U_j, T_i and, T_j by demanding that above cross-collision term correctly reproduces the momentum and energy transfers between different species. The resulting relations are

$$U_{ij}=(1-\delta_i)U_i+\delta_iU_j,$$
$$T_{ij}=T_i+\frac{2m_i}{m_i+m_j}\delta_i(T_j-T_i)+\frac{m_i\delta_i}{3\kappa}\left(\frac{2m_j}{m_i+m_j}-\delta_i\right)(U_j-U_i)^2,$$

where δ_i is a free parameter to be determined so as to satisfy further requirements. By setting the δ_i at an appropriate value, the model equation can correctly reproduce one of the transport properties such as velocity, thermal conductivity or diffusion in binary gas mixtures. In this work the δ_i is determined as

$$\delta_i=m_j/(m_i+m_j), \qquad (2)$$

which leads to the correct diffusion coefficient of binary gas mixtures. The δ_i takes a form different from Eq. (2), if one requires the correct reproduction of viscosity or thermal conductivity. In the previous work, we have examined the dependence of the solution of the model equations on the δ_i, and pointed out the solution to be insensitive to the variation in δ_i [3].

3. Computional Method

In order to make Eq. (1) tractable the new variables ξ_i and G_i are introduced as

$$\xi_i=\int^x(\nu_{ii}+\nu_{ij})dx, \qquad G_i=(\nu_{ii}M_{ii}+\nu_{ij}M_{ij})/(\nu_{ii}+\nu_{ij}).$$

In terms of ξ_i and G_i, Eq. (1) is written

$$u\partial f_i/\partial\xi_i+f_i=G_i. \tag{3}$$

The formal solution of this equation is

$$\begin{aligned} f_i(\xi_i, u\gtrless 0)&=\int_{\mp\infty}^{\xi_i}\frac{G_i(\xi_i', \boldsymbol{v})}{u}\exp\left(\frac{\xi_i'-\xi_i}{u}\right)d\xi_i' \\ &=\exp\left(\mp\frac{\Delta\xi_i}{u}\right)\int_{\mp\infty}^{\xi_i\mp\xi_i}\frac{G_i}{u}\exp\left[\frac{\xi_i'-(\xi_i\mp\Delta\xi_i)}{u}\right]d\xi_i' \\ &\quad+\int_{\xi_i\mp\Delta\xi_i}^{\xi_i}\frac{G_i}{u}\exp\left(\frac{\xi_i'-\xi_i}{u}\right)d\xi_i' \\ &=\exp(-\alpha_i)f_i(\xi_i\mp\Delta\xi_i, \boldsymbol{v})+\int_{\xi_i\mp\Delta\xi_i}^{\xi_i}\frac{G_i}{u}\exp\left(\frac{\xi_i'-\xi_i}{u}\right)d\xi_i', \end{aligned} \tag{4}$$

with $\alpha_i=\Delta\xi_i/|u|$, where $\Delta\xi_i(>0)$ is a small spatial increment. The function $G_i(\xi_i', \boldsymbol{v})$ appearing in the last expression of Eq. (4) is expanded in terms of $\xi_i'-\xi$ about $\xi_i'=\xi_i$ as

$$G_i(\xi_i', \boldsymbol{v})=\sum_{l=0}^{\infty}\frac{\partial^l G_i}{\partial\xi_i^l}\frac{(\xi_i'-\xi_i)^l}{l!}.$$

Then E. (4) becomes

$$f_i(\xi_i, u\gtrless 0)=\exp(-\alpha_i)f_i(\xi_i\mp\Delta\xi_i, \boldsymbol{v})+\sum_{l=0}^{\infty}(-u)^l H_l(\alpha_i)\frac{\partial^l G_i(\xi_i, \boldsymbol{v})}{\partial\xi_i^l} \tag{5}$$

where the function $H_l(\alpha_i)$ is defined by

$$H_l(\omega)=\frac{1}{l!}\int_0^{\omega}t^l e^{-t}dt=1-e^{-\omega}\sum_{i=0}^{l}\frac{\omega^i}{i!}.$$

The $\partial^l G_i/\partial\xi_i^l$ in Eq. (5) may be replaced by the difference quotients as

$$\left.\begin{aligned} &\partial G_i/\partial\xi_i=[G_i(\xi_i, v)-G_i(\xi_i\mp\Delta\xi_i, v)]/(\pm\Delta\xi_i),\\ &\partial^2 G_i/\partial\xi_i^2=\cdots \quad ,\\ &\cdots \quad .\end{aligned}\right\} \tag{6}$$

With the use of assumptions (6), the final equation for the distribution function is

$$\begin{aligned} f_i(\xi_i, u\gtrless 0)=&\exp(-\alpha_i)f_i(\xi_i\mp\Delta\xi_i, v)+[1-\exp(-\alpha_i)]G_i(\xi_i, v)\\ &+[(1+1/\alpha_i)\exp(-\alpha_i)-1/\alpha_i][G_i(\xi_i, v)-G_i(\xi_i\mp\Delta\xi_i, v)]. \quad (7)\\ &+\cdots \end{aligned}$$

In Eq. (7) the second and third terms of the right-hand side correspond to the terms of order $l=0$ and $l=1$, respectively, in Eq. (5).

If $G_i(\xi_i, v)$, which is a function of n_i, U_i and T_i, is primarily known, Eq. (7) provides the distribution step by step from the upstream or the downstream state. In this work an iterative procedure is employed to solve Eq. (7). With an appropriate initial guess at n_i, U_i and T_i, the distribution function is determined from Eq. (7). The n_i, U_i and T_i are re-valuated from the resulting distribution function. This procedure is iterated until a convergent solution is achieved.

It should be noted that the difference scheme (7) is not a simple first-order one, but retains an exponential nature pertinent to the distribution function. Characteristic features of the scheme (7) are described in the Appendix, especially by comparing with the simple difference equations.

The actual computations were performed using Eq. (7), in which the terms of second order or higher ($l\geq 2$) were truncated. To save the computation time and memory, Eq. (7) is integrated with respect to v and w after multiplying by 1 or (v^2+w^2) as

$$\begin{aligned} f_i^{(k)}(x, u\gtrless 0)=&\exp(-\alpha_i)f_i^{(k)}(x\mp\Delta x, u)+[1-\exp(-\alpha_i)]G_i^{(k)}(x, u)\\ &+[(1+1/\alpha_i)\exp(-\alpha_i)-1/\alpha_i][G_i^{(k)}(x, u)-G_i^{(k)}(x\mp x, u)], \quad (8)\\ &(i=1, 2,\ k=1, 2), \end{aligned}$$

where

$$\begin{bmatrix} f_i^{(1)}\\ f_i^{(2)}\end{bmatrix}=\int f_i\begin{bmatrix}1\\ v^2+w^2\end{bmatrix}dvdw, \qquad \begin{bmatrix} G_i^{(1)}\\ G_i^{(2)}\end{bmatrix}=\int G_i\begin{bmatrix}1\\ v^2+w^2\end{bmatrix}dvdw,$$

and $\alpha_i=(\nu_{ii}+\nu_{ij})\Delta x/|u|$. In Eq. (8) the original independent variable x has been used in place of ξ_i. In terms of $f_i^{(k)}$, the number density, velocity, temperature parallel to the x-axis and temperature normal to the x-axis are given, respectively, by

$$\left.\begin{aligned} &n_i=\int f_i^{(1)}du, \qquad n_iU_i=\int f_i^{(1)}udu,\\ &n_i\kappa T_{i//}/m_i=\int f_i^{(1)}(u-U_i)^2du, \qquad 2n_i\kappa T_{i\perp}/m_i=\int f_i^{(2)}du.\end{aligned}\right\} \tag{9}$$

$$T_i=(T_{i//}+2T_{i\perp})/3.$$

4. Results

For argon-helium mixtures a set of equations (8) and (9) were numerically solved. A measure of the rate of convergence was set up by examining the constancy of the number flux. In each stage of iteration, the normalized number flux $n_iU_i/(n_iU_i)_{-\infty}$ referred to the upstream state is not necessarily equal to unity. However, by proceeding with the iteration the value of the normalized number flux approaches unity throughout the shock wave structure. The iterative procedure was followed until the condition $|n_iU_i/(n_iU_i)_{-\infty}-1|_{\max}<3\times10^{-4}$ was fulfilled. Each iteration was carried out over 600～900 discrete points across the shock wave structure.

Figure 1 shows the shock wave structure for the case where the argon mole fraction $\chi_A=0.11$ and the shock Mach number $M=1.6$. The velocity is normalized as $(U_i(x)-U_{+\infty})/(U_{-\infty}-U_{+\infty})$, and the temperature as $(T_i(x)-T_{-\infty})/(T_{+\infty}-T_{-\infty})$. The mean free path is given by $L=\mu^*/\rho U$ where the viscosity coefficient μ^* refers

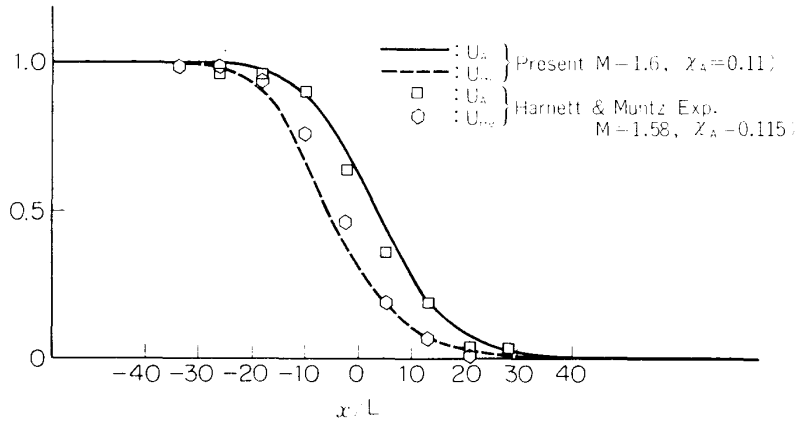

Fig. 1-1.

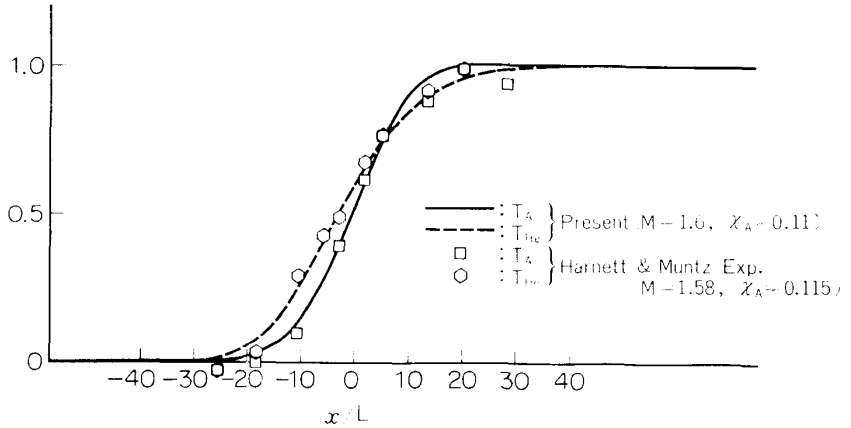

Fig. 1-2.

Fig. 1. Shock wave structure for $\chi_A=0.11$, $M=1.6$.

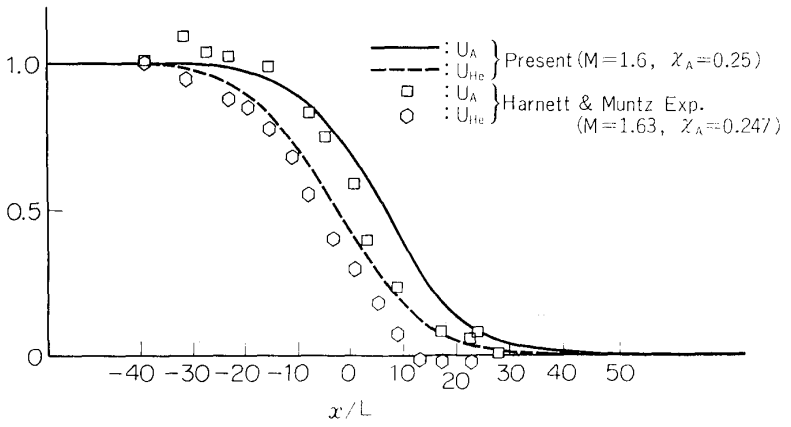

FIG. 2-1.

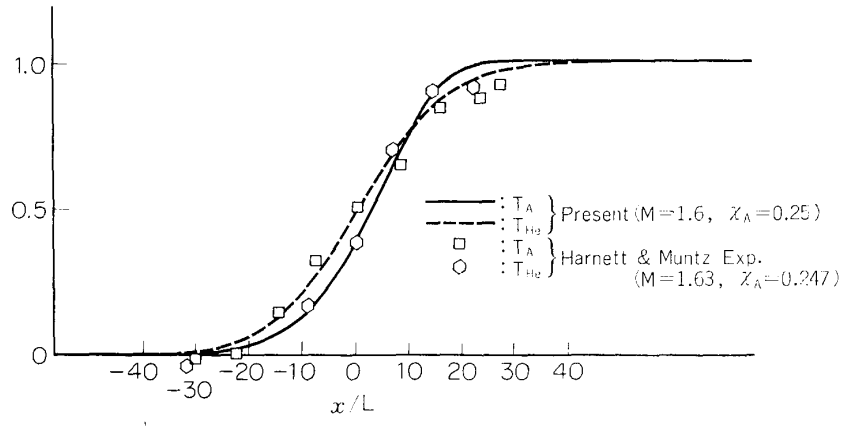

FIG. 2-2.

FIG. 2. Shock wave structure for $\chi_A=0.25$, M=1.6.

to the sonic condition of uniform flow ahead of the shock wave. The viscosity coefficient used in this work is based on that in Ref. [*13*]. Temperature T^* at the sonic condition, which needs to determine the viscosity coefficient, is given by the isentropic relation

$$\frac{T^*}{T}=\frac{2}{\gamma+1}\left(1+\frac{\gamma-1}{2}M^2\right)$$

where γ is the specific heat ratio and T the temperature at the point where the Mach number is equal to M. Figure 1 includes the experimental results by Harnett and Muntz, and indicates fairly good agreement between experiment and computation. It should be emphasized that no argon temperature overshoot appears in the computational results, as it does in the experimental results. The shock wave structure for the case $\chi_A=0.25$ and $M=1.6$ is shown in Fig. 2.

The experimental temperature profiles show that the slope of helium temperature is steeper than that of argon temperature, while the computational profiles indicate

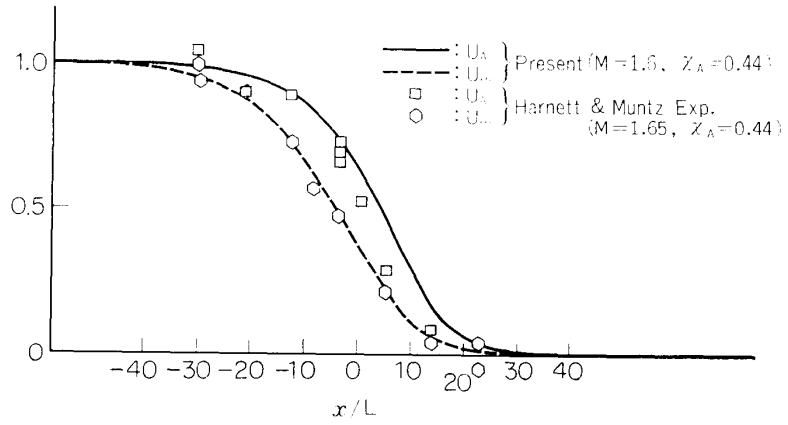

FIG. 3-1.

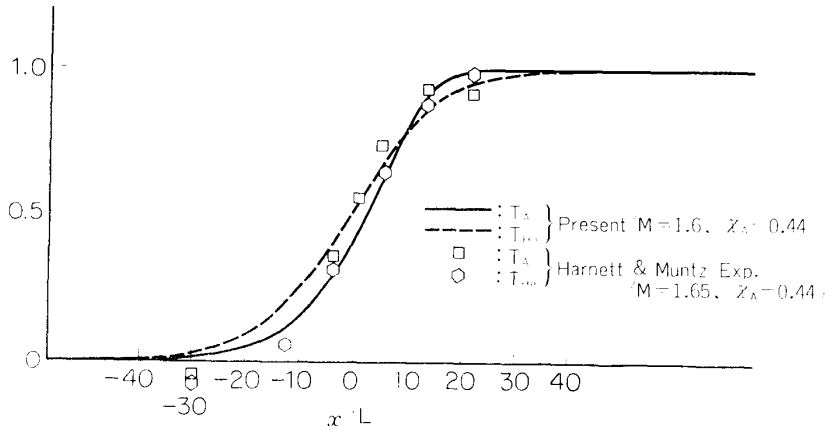

FIG. 3-2.

FIG. 3. Shock wave structure for $\chi_A=0.44$, M=1.6.

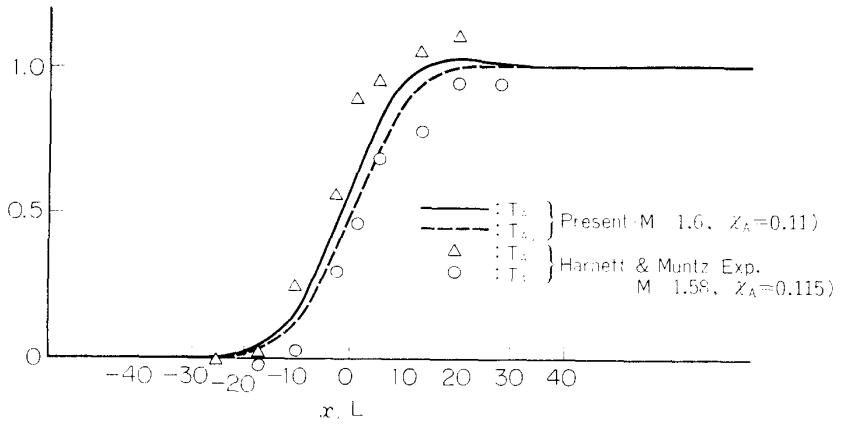

FIG. 4. Parallel and normal temperatures of argon for $\chi_A=0.11$, M=1.6.

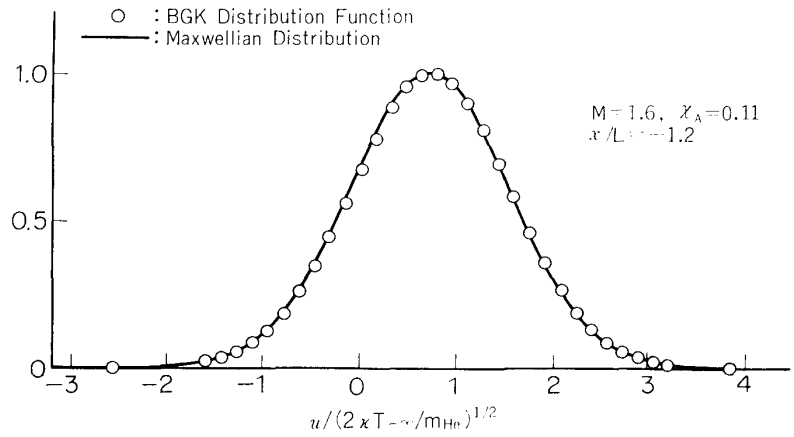

FIG. 5. Normalized distribution function of helium at the point $x/L=-1.2$ for $\chi_A=0.11$, $M=1.6$.

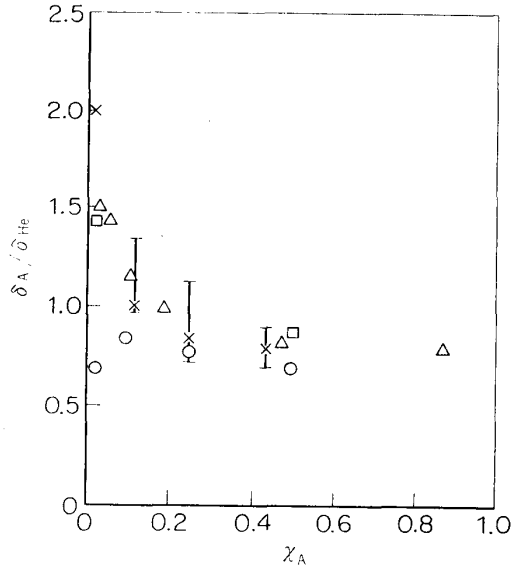

FIG. 6. Ratio of argon shock wave thickness to helium shock wave thickness. I, results of Harnett and Muntz [*10*]; △, results of Center [*8*]; ○, results of Sherman [*1*]; □, results of Bird [*5*]; ×, results of present computations. Shock wave thickness is referred to maximum slopes of density profiles.

contrast aspect. As regards this contrast, the computational temperature profiles appear to be more plausible than the experiment, because the thermal conductivity of a gas increases with decreasing particle mass of the gas, so that the profile of light gas temperature is expected to be less steeper than that of heavy gas temperature. Figure 3 shows the shock wave structure for the case $\chi_A=0.44$ and $M=1.6$.

An example of the parallel and normal temperature profiles is shown in Fig. 4 for the case $\chi_A=0.11$ and $M=1.6$. The agreement between experiment and computation is reasonable as a whole but less satisfactory compared with that for the

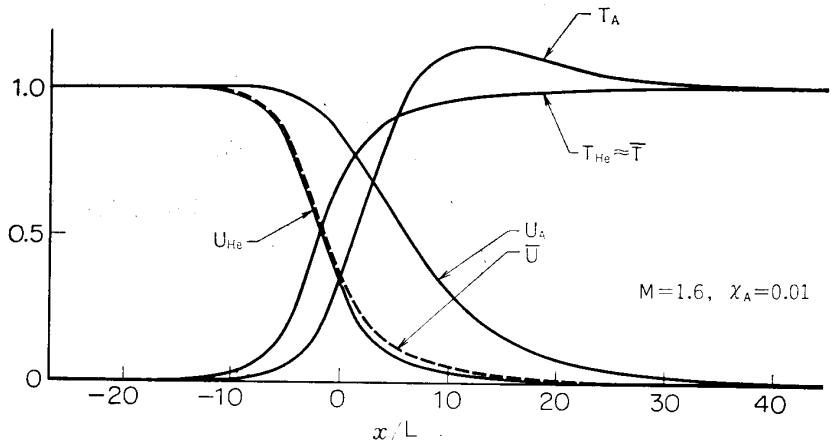

FIG. 7-1.

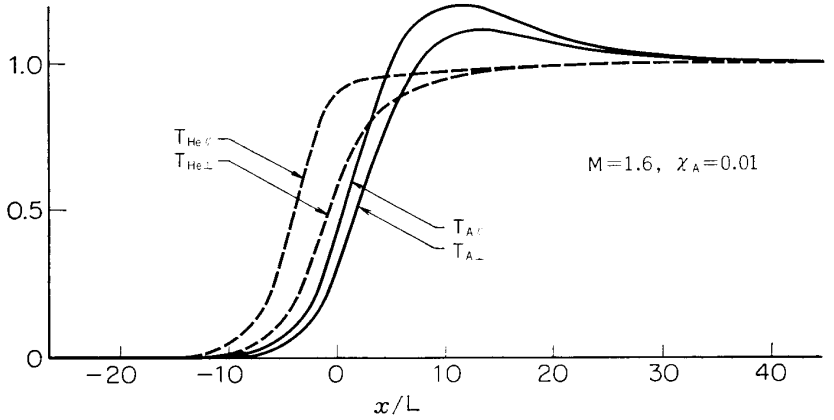

FIG. 7-2.

FIG. 7-2. Shock wave structure for $\chi_A=0.01$, $M=1.6$.

species velocities or the species total temperatures. A similar comparison between experiment and computation was also found in the argon parallel temperatures for $\chi_A=0.44$ and $M=1.6$, although the quantitative comparison was not presented here. It was found from the computational results that for both argon and helium temperatures, the parallel temperatures were always higher than the normal temperatures throughout the shock wave structures. In all the three cases noted the computational parallel temperatures never overshoot the Rankine-Hugoniot downstream value. Figure 5 shows a typical distribution function of helium for the case $\chi_A=0.11$ and $M=1.6$. Circles represent the reduced distribution function computed, and solid line represents the relevant Maxwellian distribution. The deviation of the computed distribution function from the Maxwellian is very small. A smilar trend has been noted for the case $\chi_A=0.115$ and $M=1.58$ in the experiment by Harnett and Muntz. The ratio of the maximum density slope thickness of argon shock to that of helium shock is determined from the computational results. Figure 6, in which the data are reproduced partly from Ref. [*10*], compares the present results with those of existing theories and experiments.

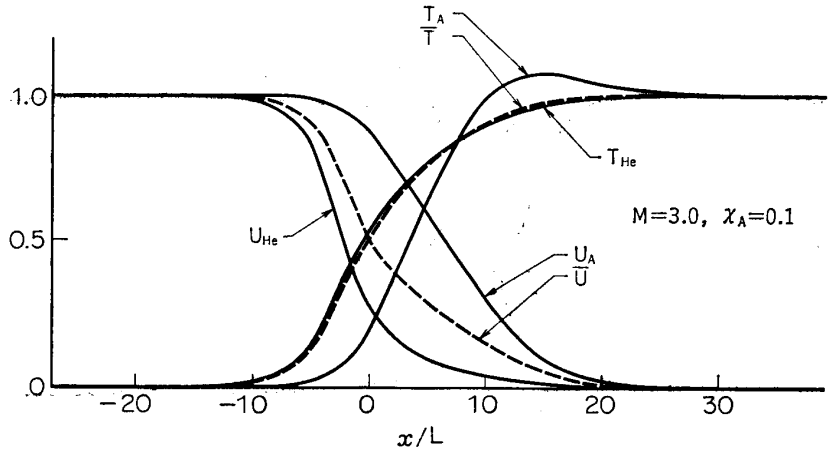

FIG. 8-1.

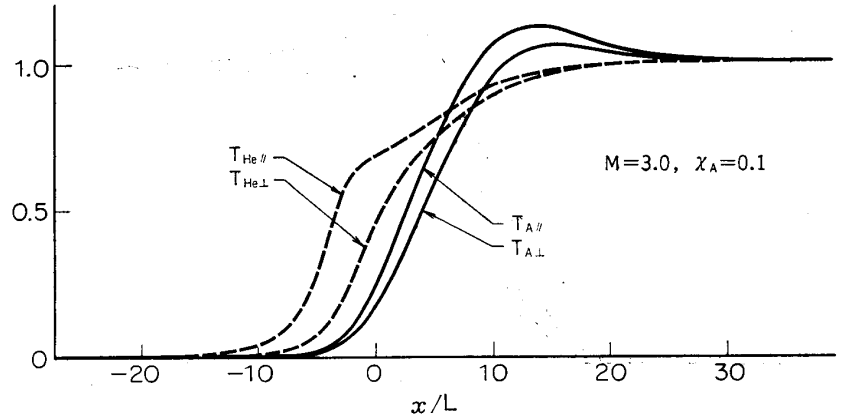

FIG. 8-2.

FIG. 8. Shock wave structure for $\chi_A=0.1$, $M=3.0$.

Further computations for the case $\chi_A=0.01$ and $M=1.6$ and for the case $\chi_A=0.1$ and $M=3.0$ were performed to clarify the temperature overshoot phenomena. Figure 7 shows the shock wave structure for the case $\chi_A=0.01$ and $M=1.6$. $\bar{U}$ and $\bar{T}$ are the averaged velocity and temperature, which are defined respectively by

$$\bar{U}=(m_A n_A U_A+m_{He}n_{He}U_{He})/(m_A n_A+m_{He}n_{He}),$$
$$\bar{T}=(n_A T_A+n_{He}T_{He})/(n_A+n_{He}).$$

Figure 7 exhibits a distinct overshoot of argon temperature, especially an overshoot of the argon parallel temperature. Figure 8 corresponds to the case $\chi_A=0.1$ and $M=3.0$, and a similar overshoot of argon temperatures occurs.

5. Concluding Remarks

In view of good agreement between experiment and computation, the kinetic model equation which is employed here can be applied in reasonable accuracy to

the problem of the shock wave structures in binary gas mixtures. The temperature overshoot of heavy gas is expected for a sufficiently small mole fraction of heavy gas. Such an overshoot is also expected to occur for a comparatively larger mole fraction of heavy gas, as the shock Mach number becomes higher.

Finally we note a physical aspect of the appearance of temperature overshoot. In the case where mole fraction of heavy gas is vanishingly small, the main structure of shock wave is determined by the light gas. This shock wave plays a role of decelerating the heavy gas, and converting the energy of ordered motion into the thermal energy. Thus, an increase in the thermal energy of heavy gas occurs within the shock wave structure due to the deceleration, while the thermal energy dissipates by conduction. Due to the slow thermal conduction of heavy gas, however the increased thermal energy could not dissipate promptly, so that an overshoot of heavy gas temperature may possibly appear.

The authors wish to thank Miss Sachiko Hatano for her invaluable assistance in the numerical computations.

Department of Aerodynamics
Institute of Space and Aeronautical Science
University of Tokyo
March 7, 1974

Appendix

In order to obtain difference equations we write Eq. (3) in the form

$$u[f_i(\xi_i, \boldsymbol{v})-f_i(\xi_i \mp \Delta\xi_i, \boldsymbol{v})]/(\mp\Delta\xi_i)+f_i(\xi_i, \boldsymbol{v})=G_i(\xi_i, \boldsymbol{v}), \qquad \text{for } u\gtrless 0,$$

or more plausibly

$$\begin{aligned} &u[f_i(\xi_i, \boldsymbol{v})-f_i(\xi_i \mp \Delta\xi_i, \boldsymbol{v})]/(\pm\Delta\xi_i)+[f_i(\xi_i, \boldsymbol{v})+f_i(\xi_i \mp \Delta\xi_i, \boldsymbol{v})]/2 \\ &\quad =[G_i(\xi_i, \boldsymbol{v})+G_i(\xi_i \mp \Delta\xi_i, \boldsymbol{v})]/2, \qquad \text{for } u\gtrless 0, \end{aligned}$$

which reduces to

$$f_i(\xi, u\gtrless 0)=\frac{1}{1+\alpha_i} f_i(\xi_i \mp \Delta\xi_i, \boldsymbol{v})+\left(1-\frac{1}{1+\alpha_i}\right)G_i(\xi_i, \boldsymbol{v}), \qquad \text{(A-1)}$$

or

$$\begin{aligned} f_i(\xi_i, u\gtrless 0)=&\frac{1-\alpha_i/2}{1+\alpha_i/2} f_i(\xi_i \mp \Delta\xi_i, \boldsymbol{v})+\left(1-\frac{1-\alpha_i/2}{1+\alpha_i/2}\right)G_i(\xi_i, \boldsymbol{v}) \\ &+\left[\left(1+\frac{1}{\alpha_i}\right)\frac{1-\alpha_i/2}{1+\alpha_i/2}-\frac{1}{\alpha_i}\right]\left[G_i(\xi_i, \boldsymbol{v})-G_i(\xi_i \mp \Delta\xi_i, \boldsymbol{v})\right], \end{aligned} \qquad \text{(A-2)}$$

If $1/(1+\alpha_i)$ in Eq. (A-1) is replaced by $\exp(-\alpha_i)$, Eq. (A-1) becomes quite same as Eq. (7) in which the terms of first order or higher are neglected. In addition, $(1-\alpha_i/2)/(1+\alpha_i/2)$ in Eq. (A-2) exactly corresponds to $\exp(-\alpha_i)$ in Eq. (7) in

which the terms of second order or higher are neglected. So long as $\alpha_i \ll 1$, $\exp(-\alpha_i) \approx 1/(1+\alpha_i) \approx (1-\alpha_i/2)/(1+\alpha_i/2)$, but for finite α_i there is an apparent difference between these functions. The present difference scheme (7), therefore, would lead to the results different from those given by a type of scheme (A–1) or (A–2). In order to evaluate the efficiency of given numerical methods, numerical computations were made using Eq. (A–1) as well as Eq. (7) for the same condition. The results obtained from Eq. (7) were favourable: these sufficiently satisfied the conservation law of mass fluxes, as was shown in the main text. In general, for the problem of shock wave structures the scheme (A–1) possesses a positive defect that for small $|u|$ the resulting distribution function $f_i(\xi_i, v)$ shows an oscillatory behavior with varying ξ_i. Such an oscillation is physically not realistic.

References

[1] F. S. Sherman: J. Fluid Mech. 8, 465 (1960).
[2] M. M. Oberai: Phys. Fluids 8, 826 (1965).
[3] K. Abe and H. Oguchi: in *Rarefied Gas Dynamics,* edited by L. Trilling and H. Y. Wachman (Academic Press, New York, 1969), Vol. I, p. 425.
[4] A. E. Beylich: Phys. Fluids **11**, 2764 (1968).
[5] G. A. Bird: J. Fluid Mech. **31**, 657 (1968).
[6] E. Goldman and L. Sirovich: J. Fluid Mech. **35**, 575 (1969).
[7] W. L. Harris and G. K. Bienkowski: in *Rarefied Gas Dynamics,* edited by L. Trilling and H. Y. Wachman (Academic Press, New York, 1969), Vol. I, p. 397.
[8] R. E. Center: Phys. Fluids **10**, 1777 (1967).
[9] D. E. Rothe: Phys. Fluids **9**, 1643 (1966).
[10] L. N. Harnett and E. P. Muntz: Phys. Fluids **15**, 565 (1972).
[11] E. P. Gross and M. Krook: Phys. Rev. **102**, 593 (1956).
[12] T. F. Morse: Phys. Fluids **7**, 2012 (1964).
[13] S. Chapman and T. G. Cowling: *Mathematical Theory of Non-Uniform Gases* (Cambridge University Press, London, 1939), Chap. 12, p. 230.